Materials Transactions, Vol. 48, No. 7 (2007) pp. 1822 to 1827
Special Issue on Bulk Metallic Glasses —Selected Papers from the Fifth International Conference on Bulk Metallic Glasses (BMGV)

Characterization of Zr-Cu Base Metallic Glasses by means of Hydrogen Internal Friction Peak

H. Mizubayashi*[1], I. Nakamura*[2], K. Yamagishi*[2] and H. Tanimoto

Institute of Materials Science, University of Tsukuba, Tsukuba 305-8573, Japan

The hydrogen internal friction peak in Zr_{50}-metallic glasses ($Zr_{50}Cu_{50}$, $Zr_{50}Cu_{40}Al_{10}$ and $Zr_{50}Cu_{35}Al_{10}Ni_5$) was studied. The hydrogen internal friction peak was shifted exponentially to lower temperatures with increasing hydrogen concentration similarly to other Zr-Cu base metallic glasses reported in the literature. The peak height increased in proportion to the square-root of hydrogen concentration. These results were discussed in the view point of the hydrogen induced structural relaxation in these metallic glasses. [doi:10.2320/matertrans.MJ200727]

(Received November 14, 2006; Accepted March 5, 2007; Published June 20, 2007)

Keywords: *metallic glass, hydrogen, internal friction, structural relaxation*

1. Introduction

Some metallic glasses can contain a large amount of hydrogen in solution, *e.g.*, late-transition-metal-early-transition-metal glasses can contain hydrogen in solution more than one hydrogen (H) per metal (M), where the maximum content depends on the chemical composition of metals (see Ref. 1) and references therein). After the finding of the hydrogen induced internal friction peak (HIFP) in metallic glasses,[2] the HIFP in various metallic glasses have intensively been studied (see Refs. 3) and 4), and references therein). The HIFP in metallic glasses is associated with the stress-induced ordering of hydrogen.[3] Although heavily hydrogenated metallic glasses are very brittle, the strengthening of metallic glasses by hydrogenation was recently found for the hydrogen concentration, C_H, below about 0.4 in H/M.[5,6] Then, the HIFP in metallic glasses has been revisited to seek a new high-damping and high-strength material,[5–17] where the peak temperature, T_p, and the peak height, $Q^{-1}{}_p$, are measures of the material performance. Experimentally, the peak temperature and the peak height of the HIFP in metallic glasses show a decrease and an increase with increasing hydrogen concentration, respectively.[3,4] As the peak height increases to the high-damping region as high as 10^{-2} the peak temperature in most metallic glasses becomes much lower than room temperature, but the peak temperature in some Zr-Cu base metallic glasses remains near room temperature. Such Zr-Cu base metallic glasses are a potential high-damping and high-strength material,[5–7] where more knowledge on the hydrogen concentration dependencies of the peak temperature and the peak height and the effect of alloying elements on these quantities is required.

Electrochemical works on binary metallic glasses have indicated that hydrogen atoms are mainly sitting on tetrahedral sites under nearest neighbor blocking and the heat of solution, G_H, for one hydrogen atom is well explained by the heat of solution, G_t, for one hydrogen atom on a tetrahedral site (the site energy, hereafter) in the wide hydrogen concentration range.[1,18] In a binary metallic glass of elements A and B, G_t may be estimated by,

$$G_t = (n_A \Delta H_A + n_B \Delta H_B)/(n_A + n_B), \tag{1}$$

where n_A and n_B are the number of A and B atoms in the tetrahedron, and ΔH_A and ΔH_B are the heat of solution for hydrogen in the pure substances A and B, respectively. A recent electrochemical work on multi-components metallic glasses has indicated that the G_H data are well explained by G_t given in eq. (1) after extension of the fractional average to multi-components alloys.[19] These electrochemical works indicate that the heat of solution for one hydrogen atom on a tetrahedral site is hardly modified by the structural relaxations inevitably induced by hydrogen charging. So far an increase in the heat of solution for one hydrogen atom with increasing hydrogen concentration is assumed to be mainly responsible for the decrease in peak temperature with increasing hydrogen concentration, where the saddle point energies on the way of diffusion jump between tetrahedra are assumed to remain unchanged by the hydrogenation (the site-energy-governing model, hereafter).[3,4,20] The site-energy-governing model predicts that the HIFP shows monotonic growth with increasing hydrogen concentration, where the peak temperature remains almost unchanged before filling up of the tetrahedral sites with the lowest G_t, *e.g.*, the Zr_4 sites in Zr-Cu metallic glasses, and then starts to decrease with filling of the tetrahedral sites with higher G_t. On the other hand, a recent HIFP work indicates that for several Zu-Cu base metallic glasses, the hydrogen concentration dependence of peak temperature can be well described by,

$$T_p = \Delta T_p \exp(-C_H/\tau_H) + T_{p0}, \tag{2}$$

where ΔT_p denotes a variation range of the peak temperature, τ_H is the hydrogen concentration at where a change in peak temperature becomes $\Delta T_p \exp(-1)$ and T_{p0} is the ultimate value of T_p.[15,21] The site-energy-governing model mentioned above cannot explain the observed relationship (2). It is indicated that the hydrogen induced structural relaxation (HISR) plays the major role on the relationship (2) observed for the HIFP in Zu-Cu base metallic glasses. In the present work, the effects of alloying elements on the hydrogen concentration dependences of the peak temperature and the

*[1]Corresponding author, E-mail: mizuh@ims.tsukuba.ac.jp
*[2]Graduate Student, University of Tsukuba

peak height were studied for Zr_{50}-Cu base metallic glasses in the view point of HISR.

2. Experimental

Alloy ingots were prepared by arc-melting. Ribbon specimens of $Zr_{50}Cu_{40}Al_{10}$ and $Zr_{50}Cu_{35}Al_{10}Ni_5$ metallic glasses were prepared by melt spinning in a high-purity Ar gas atmosphere, where the thickness and the width of ribbons were about 30 µm and 1 mm, respectively. The specimen surfaces were polished mechanically in water avoiding heating up during polishing to remove a surface layer and to smoothen. Hydrogen charging was made electrolytically in 0.1 N H_2SO_4 solution at room temperature. The hydrogen charged specimen was aged for a few days at room temperature before measurements to homogenize the hydrogen distribution in the specimen. The internal friction, Q^{-1}, and the resonant frequency were measured by means of the vibrating reed method at about 300 Hz and the strain amplitude of 10^{-6}. The internal friction measurements were conducted in the temperature range between 80 K and 400 K. A change in the specimen length, $\Delta L/L_0$, due to the hydrogenation was measured by an optical microscope with a micrometer stage. The volume expansion, $\Delta V/V_0$, of a specimen was determined by assuming the relationship of $\Delta V/V_0 = 3\Delta L/L_0$. The X-ray diffraction measurements were made by the conventional θ-2θ scan using the Cu Kα radiation. The hydrogen concentration was determined by the thermal desorption method.[22]

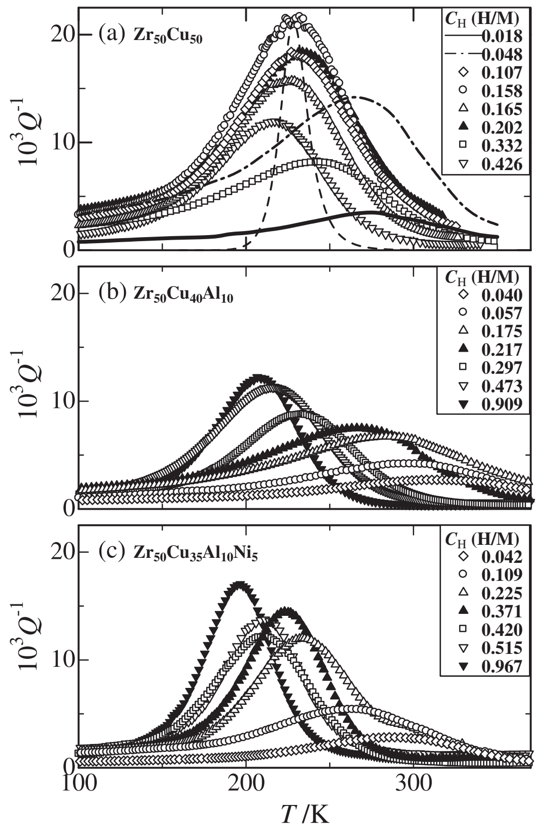

Fig. 1 Examples of the HIFP observed at about 300 Hz: (a) $Zr_{50}Cu_{50}$,[23] (b) $Zr_{50}Cu_{40}Al_{10}$, and (c) $Zr_{50}Cu_{35}Al_{10}Ni_5$. The dashed curve in (a) denotes a theoretical Debye peak with $\tau_0 = 1.1 \times 10^{-17}$ s and $E = 0.62$ eV reported for $Zr_{50}Cu_{50}$.[23]

3. Results

Figures 1(a) to 1(c) show examples of the HIFP observed at $\sim$300 Hz in $Zr_{50}Cu_{50}$,[23] $Zr_{50}Cu_{40}Al_{10}$ and $Zr_{50}Cu_{35}Al_{10}Ni_5$ (Zr_{50}-metallic glasses, and so on) with various hydrogen concentration, respectively. As seen in Fig. 1(a), the HIFP in Zr_{50}-metallic glasses is much broader than a theoretical Debye peak and accompanied with a low temperature tail, indicating that the activation energy, E_H, for the hydrogen diffusion shows a wide distribution. With increasing hydrogen concentration, the HIFP in Zr_{50}-metallic glasses moved to lower temperatures as a whole, where a decrease in peak temperature followed by saturation and an increase in peak height followed by a tendency of saturation with increasing hydrogen concentration were commonly observed except for the detailed variations among metallic glasses. Figure 2(a) shows examples of the temperature dependence of the resonant frequency, f, observed for $Zr_{50}Cu_{40}Al_{10}$, where the observed resonant frequency is normalized to its value at about 80 K, f_0, ($f_0 \sim 300$ Hz, here). A change in f/f_0 found between $\sim$80 K and $\sim$380 K, $|\Delta f_{80\text{–}380\,K}/f_0|$, is determined from the f/f_0 *vs.* T data shown in Fig. 2(a). The corresponding change in Young's modulus, $|\Delta M_{80\text{–}380\,K}/M|$, is estimated as twice of $|\Delta f_{80\text{–}380\,K}/f_0|$. In Fig. 2(b), the $|\Delta M_{80\text{–}380\,K}/M|$ *vs.* C_H data are shown (see the left scale). For hydrogenated specimens, $|\Delta M_{80\text{–}380\,K}/M|$ is composed of the intrinsic temperature change in the Young's modulus, $|\Delta M_T/M|$, and the modulus defect associated with the HIFP, $|\Delta M_R/M|$. In Fig. 2(b), $|\Delta M_T/M|$ is assumed to remain constant in the whole hydrogen concentration range (the dashed line) and then $|\Delta M_R/M|$ (the right scale) is estimated after subtraction of $|\Delta M_T/M|$. Figure 2(c) shows the $|\Delta M_R/M|$ *vs.* $Q^{-1}{}_p$ data observed for $Zr_{50}Cu_{50}$,[23] $Zr_{50}Cu_{40}Al_{10}$, and $Zr_{50}Cu_{35}Al_{10}Ni_5$. The linear relationship between these quantities is commonly observed but the observed ratios of $|\Delta M_R/M|$ to $Q^{-1}{}_p$ are much larger than two expected for a single relaxation peak. It is noted that the relaxation strength estimated after the decomposition of the HIFP into the constituent single-relaxation peaks shows good agreement with $|\Delta M_R/M|$.[23,24] That is, the peak height is indicative of the relaxation strength of the HIFP. The XRD measurements detected no crystalline phases in the present hydrogen concentration range (not shown here).

Figure 3(a) shows examples of the hydrogen concentration dependence of the peak temperature observed for Zr-Cu base metallic glasses, where the peak temperature decreased steeply in the low hydrogen concentration range and showed saturation to about 210 K in the high hydrogen concentration range. The observed hydrogen concentration dependence of peak temperature is well described by eq. (2), and redrawn on the $\ln(T_p - T_{p0})$ *vs.* C_H plot in Figures 3(b) and 3(c), where the linear relationships between $\ln(T_p - T_{p0})$ and C_H are seen. The parameters, ΔT_p, τ_H and T_{p0}, found for the observed data and the reported data[5,6,21,23–27] for the various metallic glasses are shown in Figs. 4(a) and (b), where ΔT_p and T_{p0} are plotted against τ_H, respectively. T_{p0} is almost the same in Zr_{40}-, $Zr_{50(55)}$- and Zr_{60}-metallic glasses, *i.e.* near 210 K. τ_H increases in the order of Zr_{60}-, Zr_{40}- and $Zr_{50(55)}$-

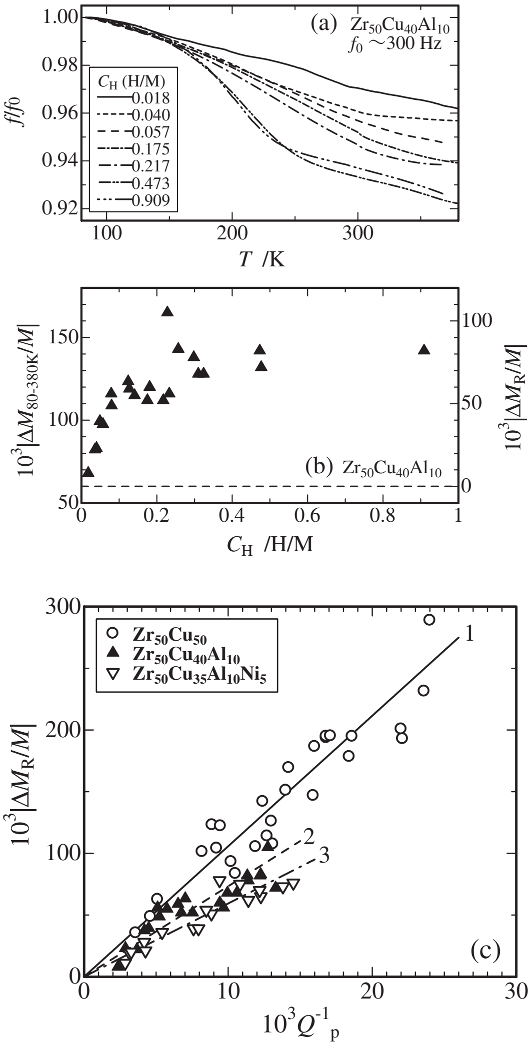

Fig. 2 (a) Examples of the f/f_0 *vs.* T data and (b) the $|\Delta M_{80\text{–}380\,\mathrm{K}}/M|$ (the left scale) and $|\Delta M_\mathrm{R}/M|$ (the right scale) *vs.* C_H data observed for $Zr_{50}Cu_{40}Al_{10}$ (see text for details). (c) The $|\Delta M_\mathrm{R}/M|$ *vs.* $Q^{-1}{}_\mathrm{p}$ data observed for $Zr_{50}Cu_{50}$,[23] $Zr_{50}Cu_{40}Al_{10}$, and $Zr_{50}Cu_{35}Al_{10}Ni_5$. The lines 1 to 3 are drawn to guide eyes.

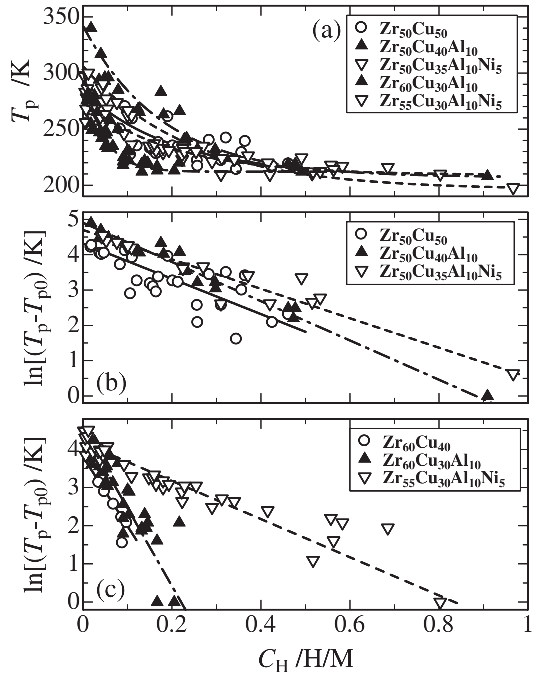

Fig. 3 (a) Examples of the hydrogen concentration dependence of the peak temperature observed for Zr-Cu-base metallic glasses. The $\ln(T_\mathrm{p} - T_{\mathrm{p}0})$ *vs.* C_H plots for (b) $Zr_{50}Cu_{50}$,[23] $Zr_{50}Cu_{40}Al_{10}$ and $Zr_{50}Cu_{35}Al_{10}Ni_5$, and (c) $Zr_{60}Cu_{40}$,[5] $Zr_{60}Cu_{30}Al_{10}$[5,6] and $Zr_{55}Cu_{30}Al_{10}Ni_5$.[21]

metallic glasses. ΔT_p for the binary metallic glasses increases in the order of Zr_{60}-, $Zr_{50(55)}$- and Zr_{40}-metallic glasses. The ultimate value of the peak temperature ($T_{\mathrm{p}0}$) is higher in Zr-Cu base metallic glasses than in Zr-Co, Zr-Ni, Ti-Ni metallic glasses.

Figure 5(a) shows the hydrogen concentration dependence of the peak height observed for $Zr_{50}Cu_{35}Al_{10}Ni_5$, and Figures 5(b) and 5(c) show the $\log Q^{-1}{}_\mathrm{p}$ *vs.* $\log(C_\mathrm{H}/\tau_\mathrm{H})$ plot for $Zr_{50(55)}$- and Zr_{60}-metallic glasses. Except for $Zr_{50}Cu_{50}$, the hydrogen concentration dependence of the peak height can be described by the relationship,

$$Q^{-1}{}_\mathrm{p} = \Delta Q^{-1}{}_\mathrm{p}(C_\mathrm{H}/\tau_\mathrm{H})^{1/2}, \tag{3}$$

where $\Delta Q^{-1}{}_\mathrm{p}$ is a measure of the relaxation strength of the HIFP. For $Zr_{60}Cu_{30}Al_{10}$, some specimens showed a strong HIFP in the as-quenched state.

Hydrogenation causes a volume expansion, $\Delta V/V_0$, of a specimen which may modify the local atomic structures in a metallic glass. Figure 6(a) shows the $\Delta V/V_0$ *vs.* C_H data observed for $Zr_{50}Cu_{35}Al_{10}Ni_5$, where the solid curve 11 is

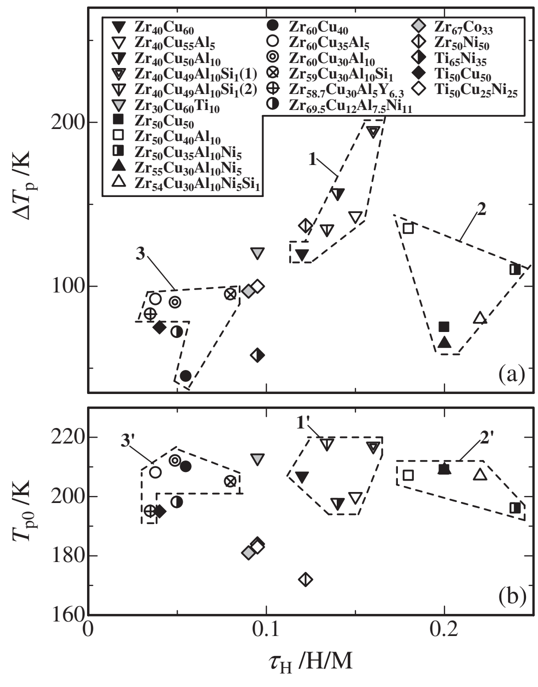

Fig. 4 The parameters, ΔT_p, $T_{\mathrm{p},0}$ and τ_H found for the Zr-base and Ti-base metallic glasses are shown, here, ΔT_p and $T_{\mathrm{p},0}$ are plotted against τ_H. The parameters for $Zr_{67}Co_{33}$,[25] $Ti_{50}Cu_{25}Ni_{25}$[26] and $Zr_{69.5}Cu_{12}Al_{7.5}Ni_{11}$[27] are found after the application of eq. (2) to the reported data. For $Zr_{40}Cu_{49}Al_{10}Si_1$, (1) and (2) denote as-quenched specimens and specimens after annealing at 400 K, respectively. 1,1′; Zr_{40}-metallic glasses, 2,2′; $Zr_{50(55)}$-metallic glasses, 3,3′; Zr_{60}-metallic glasses.

fitted to the data points. Figure 6(b) shows the $\Delta V/V_0$ *vs.* C_H data observed for Zr-metallic glasses together with those reported in the literatures.[7,22,28–32] The expansion rate,

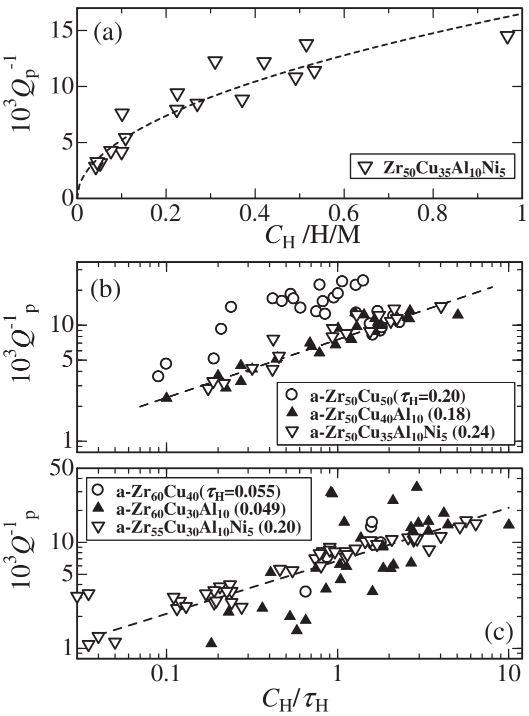

Fig. 5 (a) The hydrogen concentration dependence of the peak height, observed for $Zr_{50}Cu_{35}Al_{10}Ni_5$. The $\log Q^{-1}{}_p$ *vs.* $\log(C_H/\tau_H)$ plot for (b) $Zr_{50}Cu_{50}$, $Zr_{50}Cu_{40}Al_{10}$ and $Zr_{50}Cu_{35}Al_{10}Ni_5$, and (c) $Zr_{60}Cu_{40}$, Zr_{60}-$Cu_{30}Al_{10}$ and $Zr_{55}Cu_{30}Al_{10}Ni_5$. Dashed lines are drawn to guide eyes assuming the relationships of $10^3Q^{-1}{}_P = 16.5(C_H)^{1/2}$ in (a), $10^3Q^{-1}{}_P = 7.5(C_H/\tau_H)^{1/2}$ in (b), and $10^3Q^{-1}{}_P = 6.7(C_H/\tau_H)^{1/2}$ in (c).

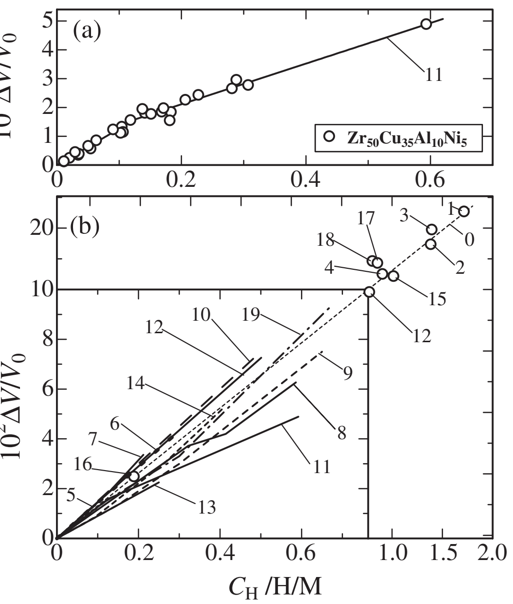

Fig. 6 (a) The $\Delta V/V_0$ *vs.* C_H data observed for $Zr_{50}Cu_{35}Al_{10}Ni_5$. The solid curve 11 is fitted to the data points and redrawn in (b). (b) The $\Delta V/V_0$ *vs.* C_H data. 1: $Zr_{76}Fe_{24}$,[28] 2: $Zr_{75}Rh_{25}$,[29] 3: $Zr_{67}Ni_{33}$,[30] 4: $Zr_{67}Pd_{33}$,[29] 5: $Zr_{60}Cu_{40}$,[7] 6: $Zr_{60}Cu_{35}A_{l5}$,[7] 7: $Zr_{60}Cu_{30}Al_{10}$,[7] 8: $Zr_{55}Cu_{30}Al_{10}Ni_5$, 9: $Zr_{50}Cu_{50}$,[22] 10: $Zr_{50}Cu_{40}Al_{10}$, 11: $Zr_{50}Cu_{35}Al_{10}Ni_5$, 12: $Zr_{50}Ni_{50}$, 13: $Zr_{40}Cu_{50}Al_{10}$, 14: $Zr_{40}Cu_{49}Al_{10}Si_1$, 15: $Zr_{41}Ni_{59}$,[31] 16: $Zr_{36}Ni_{64}$,[32] 17: $Zr_{36}Ni_{64}$,[31] 18: $Zr_{33}Ni_{67}$,[31] 19: $Ti_{50}Cu_{50}$,[22] The line 0 is drawn to guide eyes.

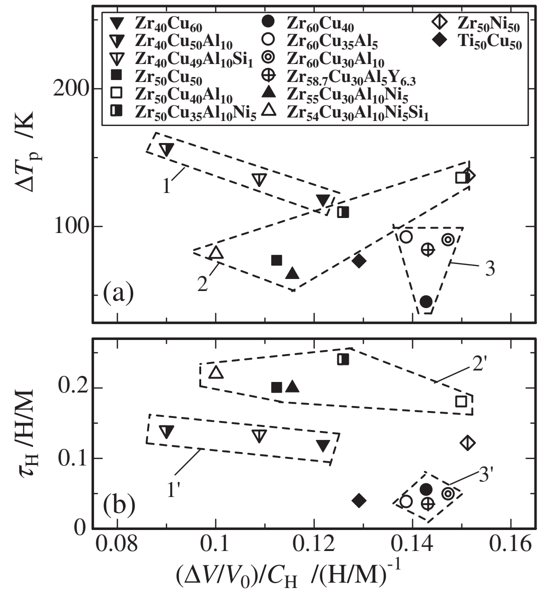

Fig. 7 The τ_H *vs.* $\Delta V/V_0$ data observed for Zr-Cu base metallic glasses and some Zr-base and Ti-base metallic glasses. 1,1′; Zr_{40}-metallic glasses, 2,2′; $Zr_{50(55)}$-metallic glasses, 3,3′; Zr_{60}-metallic glasses.

$(\Delta V/V_0)/C_H$, is a function of the alloy compositions and hydrogen concentration. In Figs. 7(a) and 7(b), ΔT_p and τ_H are plotted against the expansion rate, respectively, where the expansion rate has been evaluated for $C_H < \tau_H$. As seen in Figs. 7(a) and 7(b), the alloy composition dependencies of ΔT_p and τ_H are not well correlated with the expansion rate.

4. Discussion

As already mentioned, for Zr-Cu metallic glasses the site-energy-governing model and the electrochemical work predict that the peak temperature remains almost unchanged before filling up of the Zr_4 sites and then starts to decrease with the subsequent filling of the Zr_3Cu_1, Zr_2Cu_2 and Zr_1Cu_3 sites, where the HIFP shows a monotonic growth. In contrast, the followings were observed (see Figs. 3(a) to 3(c) and Figs. 5(a) to 5(c)). The decrease in peak temperature was steeper in the lower hydrogen concentration range and the decreasing rate in the low hydrogen concentration range was higher for Zr_{60}-metallic glasses than in Zr_{50}-metallic glasses. The HIFP showed a shift to the lower temperature side as a whole and the peak height tended toward saturation with increasing hydrogen concentration. Quantitatively, the relationships (2) and (3) were found for the peak temperature and the peak height, respectively. The site-energy-governing model cannot explain the observed results for Zr-Cu metallic glasses. For $Zr_{40}Cu_{60}$ metallic glass,[33] the hydrogen concentration dependences of the thermal desorption spectra and the onset temperature for precipitation of crystalline ZrH_2 suggest that HISR proceeds with increasing hydrogen concentration. The combination of these results suggests that the relationships (2) and (3) found for Zr-Cu-based metallic glasses are associated with HISR. Then, the saturation of peak temperature at T_{p0} indicates that HISR shows the completion in the high hydrogen concentration range, and ΔT_p is a measure of difference between the glass

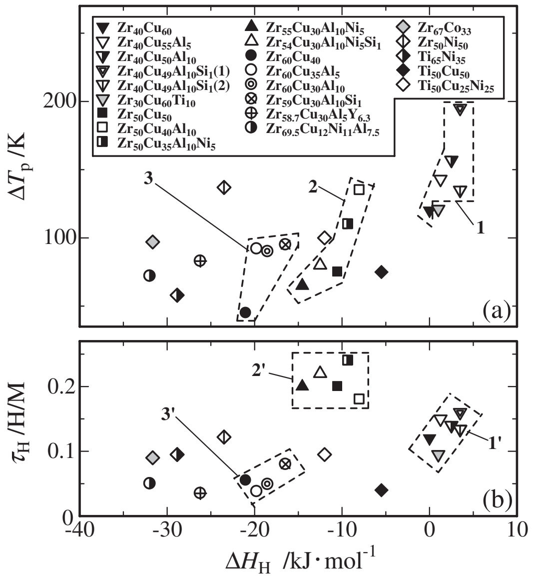

Fig. 8 (a) The ΔT_p *vs.* ΔH_H data and (b) the τ_H *vs.* ΔH_H data observed for Zr-Cu base metallic glasses and some Zr-base and Ti-base metallic glasses. 1,1′; Zr_{40}-metallic glasses, 2,2′; $Zr_{50(55)}$-metallic glasses, 3,3′; Zr_{60}-metallic glasses.

structure in the as quenched state and the ultimate glass structure after HISR. As already mentioned, the peak temperature is a measure of the activation energy of hydrogen diffusion (E_H) in the major local atomic structures, and the site energies are hardly modified by hydrogenation in multi-component metallic glasses either.[19] Thus it is suggested that the saddle point energies on the way of diffusion jump between tetrahedra are modified by HISR. On the other hand, the alloy composition dependences of ΔT_p is not well correlated with the expansion rate (see Fig. 7(a)), indicating that the saddle point energies are hardly modified by the volume expansion. τ_H is not well correlated either with the expansion rate (see Fig. 7(b)).

In Figs. 8(a) and 8(b), ΔT_p and τ_H are respectively plotted against the heat of solution of hydrogen in metallic glasses, ΔH_H, which is evaluated as the fractional average from the heat of solution data reported for element crystals and the chemical compositions of metallic glasses. For a metallic glass $A_aB_b\cdots X_x$ $(a + b + \cdots + x = 100)$ composed of elements A, B, $\cdots$, and X, ΔH_H is assumed to be expressed as

$$\Delta H_H = [a(\Delta H_A) + b(\Delta H_B) + \cdots + x(\Delta H_X)]/100, \quad (4)$$

where ΔH_A denotes the heat of solution in the element A and so on. For binary metallic glasses, ΔT_p increases with increasing heat of solution of hydrogen in metallic glasses, *i.e.*, in the order of $Zr_{60}Cu_{40}$, $Zr_{50}Cu_{50}$, and $Zr_{40}Cu_{60}$. For an effect of alloying with Al and Ni in Zr_{40}-, $Zr_{50(55)}$- and Zr_{60}-metallic glasses, ΔT_p increases with increasing heat of solution of hydrogen in metallic glasses too. The increase in ΔT_p with increasing heat of solution of hydrogen in metallic glasses indicates that the saddle point energy on the way of diffusion jump between tetrahedra increases more strongly than the heat of solution for one hydrogen atom on a tetrahedral site (G_t) by alloying of elements with low hydrogen affinity. HISR plays the major role in the observed hydrogen concentration dependence of the peak temperature, the relationship (2), observed for Zu-Cu base metallic glasses, *i.e.*, τ_H is a measure of the tolerance against HISR. Both the values of τ_H found in $Zr_{50}Cu_{40}Al_{10}$ and $Zr_{50}Cu_{35}Al_{10}Ni_5$ are very similar to τ_H found in $Zr_{50}Cu_{50}$, suggesting that τ_H is hardly modified by alloying with Al and Ni in the present composition range. A similar effect of alloying on τ_H is seen in Zr_{60}-metallic glasses and Zr_{40}-metallic glasses too. τ_H is the largest in Zr_{50}-metallic glasses. On the other hand, in general, both ΔT_p and τ_H are the smallest in Zr_{60}-metallic glasses, suggesting that the amorphous structures in Zr_{60}-metallic glasses are not far from the relaxed ones.

For the Snoek relaxation process in a crystalline solid,[34] the relaxation strength, S_H, increases proportionally to the molar concentration of the defect or the solute atom concerned when the elastic distortion around the defect or the solute atom remains unchanged, where the relationship of $Q^{-1}{}_p = S_H/2$ is expected for a single relaxation process. The elastic distortion around a hydrogen atom in a metallic glass may vary among hydrogen atoms, however, the mean elastic distortion responsible for the HIFP may be found. The observed relationship (3) indicates that the mean anisotropic distortions of tetrahedra may relax towards isotropic distortions with increasing volume expansion.

5. Conclusion

For Zr-Cu base metallic glasses, the peak temperature (T_p) of the hydrogen internal friction peak (HIFP) has been reported to shift exponentially to lower temperatures with increasing hydrogen concentration (C_H) as $T_p = \Delta T_p \exp(-C_H/\tau_H) + T_{p0}$. This means that the hydrogen concentration dependence of the peak temperature is governed not by the hydrogen site energies but by the hydrogen induced structural relaxation (HISR). T_{p0} is commonly found to be around 210 K, indicating that the local atomic structures after the completion of HISR are similar in the Zr-Cu base metallic glasses. In the present work, effects of alloying with Al and Ni on ΔT_p and τ_H were studied for Zr_{50}-metallic glasses ($Zr_{50}Cu_{50}$, $Zr_{50}Cu_{40}Al_{10}$ and $Zr_{50}Cu_{35}Al_{10}Ni_5$) and the observed results were discussed together with the effects of alloying reported for Zr_{60}-, Zr_{55}- and Zr_{40}-metallic glasses. The followings were found for ΔT_p and τ_H. For binary metallic glasses, ΔT_p increases with increasing heat of solution of hydrogen in metallic glasses, *i.e.*, in the order of $Zr_{60}Cu_{40}$, $Zr_{50}Cu_{50}$ and $Zr_{40}Cu_{60}$. For an effect of alloying with Al and Ni in Zr_{40}-, $Zr_{50(55)}$- and Zr_{60}-metallic glasses, ΔT_p increases with increasing heat of solution of hydrogen in metallic glasses too. It is indicated that the saddle point energy on the way of diffusion jump between tetrahedra increases more strongly than the heat of solution for one hydrogen atom on a tetrahedral site by alloying of elements with low hydrogen affinity. On the other hand, τ_H is hardly modified by alloying with Al and Ni for Zr_{50}-metallic glasses. A similar effect of alloying on τ_H is seen in Zr_{60}-, Zr_{55}- and Zr_{40}-metallic glasses too. τ_H increases in the order of Zr_{60}-, Zr_{40}- and $Zr_{50(55)}$-metallic glasses. Further, the hydrogen concentration dependence of the height of the HIFP ($Q^{-1}{}_p$) was found to be described by the relationship, $Q^{-1}{}_p = \Delta Q^{-1}{}_p(C_H/\tau_H)^{1/2}$, indicating that the anisotropic distortions of tetrahedra relaxed towards isotropic distortions with increasing volume expansion.

Acknowledgement

This work is partly supported by a Grant in Aid for Scientific Research and the 21st Century Center of Excellence Program from the Ministry of Education, Culture, Sports, Science and Technology, Japan.

REFERENCES

1) J. H. Harris, W. A. Curtin and M. A. Tenhover: Phys. Rev. B **36** (1987) 5784–5797.
2) B. S. Berry, W. C. Pritchet and C. C. Tsuei: Phys. Rev. Lett. **41** (1978) 410–413.
3) B. S. Berry and W. C. Pritchet: *Hydrogen in Disordered and Amorphous Solids*, G. Bambakidis and R. C. Bowman, Jr. (Eds.) (Plenum Press, New York, 1986) pp. 215–236.
4) H.-R. Sinning: J. Alloys and Compd. **310** (2000) 224–228.
5) H. Mizubayashi, S. Murayama and H. Tanimoto: J. Alloys and Compd. **330–332** (2002) 389–392.
6) H. Mizubayashi, Y. Ishikawa and H. Tanimoto: Mater. Trans. **43** (2002) 2662–2669.
7) H. Mizubayashi, Y. Ishikawa and H. Tanimoto: J. Alloys and Compd. **355** (2003) 31–36.
8) M. Hasegawa, S. Yamamura, H. Kato, K. Amiya, N. Nishiyama and A. Inoue: J. Alloys and Compd. **355** (2004) 37–41.
9) M. Hasegawa, K. Kotani, S. Yamaura, H. Kato, I. Kodama and A. Inoue: J. Alloys and Compd. **365** (2004) 221–227.
10) M. Hasegawa, M. Takeuchi, H. Kato, S. Yamaura and A. Inoue: J. Alloys and Compd. **372** (2004) 116–120.
11) M. Hasegawa, M. Takeuchi, H. Kato and A. Inoue: Acta Mater. **52** (2004) 1799–1806.
12) T. Yagi, T. Imai, R. Tamura and S. Takeuchi: Mater. Sci. Eng. A **370** (2004) 264–267.
13) H. Mizubayashi, Y. Ishikawa and H. Tanimoto: Mater. Sci. Eng. A **370** (2004) 546–549.
14) M. Hasegawa, M. Takeuchi and A. Inoue: Acta Mater. **53** (2005) 5297–5304.
15) H. Mizubayashi, K. Yamagishi and H. Tanimoto: Key Eng. Mater. **319** (2006) 133–138.
16) M. Hsegawa, M. Takeuchi, D. Nagata, T. Wada, H. Kato, Y. Yamaura and A. Inoue: Key Eng. Mater. **319** (2006) 139–144.
17) Y. Hiki, M. Tanahashi and S. Takeuchi: Key Eng. Mater. **319** (2006) 151–156.
18) R. Kirchheim, F. Sommer and G. Schluckebier: Acta Mater. **30** (1982) 1059–1068.
19) J. Bankmann, A. Pundt and R. Kirchheim: J. Alloys and Compd. **356–357** (2003) 566–569.
20) R. Kirchheim: Acta Mater. **30** (1982) 1069–1078.
21) K. Yamagishi, H. Tanimoto and H. Mizubayashi: Mater. Sci. Eng. A **422** (2006) 292–296.
22) H. Mizubayashi, M. Shibasaki and S. Murayama: Acta Mater. **47** (1999) 3331–3338.
23) H. Mizubayashi, T. Naruse and S. Okuda: Phys. Stat. Sol. (a) **132** (1992) 79–90.
24) H. Mizubayashi, H. Agari and S. Okuda: Phys. Stat. Sol. (a) **122** (1990) 221–233.
25) H.-R. Sinning: Phys. Stat. Sol. A **140** (1993) 97–108.
26) S. Yamaura, M. Hasegawa, H. Kimura and A. Inoue: Mater. Trans. JIM **43** (2002) 2543–2547.
27) H.-R. Sinning, R. Scarfone and I. S. Golovin: Mater. Sci. Engng. A **370** (2004) 78–82.
28) A. J. Maeland: *Rapidly Quenched Metals*, S. Steeb and H. Warlimont (Eds.), (Elsevier, Amsterdam, 1985) p. 1507.
29) K. Samwer and W. L. Johnson: Phys. Rev. B. **28** (1983) 2907–2913.
30) K. Aoki, A. Horata and T. Matsumoto: Proc. 4th Int. Conf. on Rapidly Quenched Metals, T. Matsumoto and K. Suzuki (Eds.), (Japan Inst. Metal, Sendai, 1982) pp. 1649–1652.
31) L. K. Varga, K. Tompa, A. Lovas, J. M. Jobert and A. Percheron-Guegan: Int. J. Hydrogen Energy **21** (1996) 927–930.
32) S. Hatta, J. Nishioka and T. Mizoguch: Proc. 4th Int. Conf. on Rapidly Quenched Metals, T. Matsumoto and K. Suzuki (Eds.), (Japan Inst. Metal, Sendai, 1982) pp. 1613–1616.
33) M. Matsumoto, H. Mizubayashi and S. Okuda: Acta Metall. Mater. **43** (1995) 1109–1117.
34) A. S. Nowick and B. S. Berry: *Anelastic Relaxation in Crystalline Solids*, (Academic Press, New York and London, 1972) p. 225.